REVIEW ARTICLE
PUBLISHED ONLINE: 30 SEPTEMBER 2010 | DOI: 10.1038/NPHOTON.2010.184

nature photonics

# Liquid-crystal lasers

Harry Coles* and Stephen Morris

**Liquid-crystal lasers are a burgeoning area in the field of soft-matter photonics that may herald a new era of ultrathin, highly versatile laser sources. Such lasers encompass a multitude of remarkable features, including wideband tunability, large coherence area and, in some cases, multidirectional emission. They have the potential to combine large output powers with miniature cavity dimensions — two properties that have traditionally been incompatible. Their potential applications are diverse, ranging from miniature medical diagnostic tools to large-area holographic laser displays. Here we discuss the scientific origins of this technology and give a brief synopsis of the cutting-edge research currently being carried out worldwide.**

Liquid crystals have become ubiquitous in everyday applications ranging from miniature mobile telephones to high-definition flat-panel displays. Such technologies are based on the reorientation of a liquid-crystal material in response to applied electric fields, which results in a change in its observed optical properties[1]. The majority of present commercial displays are based on liquid crystals exhibiting a nematic phase — the least ordered mesophase. However, materials similar to the cholesterol derivatives studied by Austrian botanist Frederick Reinitzer when he identified the liquid-crystal phase in 1888[2] have recently caused a scientific revolution in a very different field — that of tunable organic lasers.

Fundamentally, the key feature that these materials possess is the existence of a photonic bandgap for visible light. Photonic band structures have attracted considerable attention in recent years because of their ability to control the propagation of light at a range of different frequencies. This photonic bandgap is analogous to the separation of electronic bands in semiconductors, and can exist in one-, two- or three-dimensional periodic dielectric structures, depending on the number of directions in which the periodicity exists. Inside the bandgap, emission is suppressed because the density of photon states diverges at the edges of the bandgap, which leads to long photon-dwell times. Lasing from liquid-crystal media, a subject first reported[3] and patented[4] some thirty years ago, has been revisited as a result of the pioneering theoretical work of Yablonovitch[5] and John[6], who realized the remarkable optical phenomena associated with a photonic bandgap. Dowling and co-workers later showed theoretically that, owing to the sudden divergence in the density of photon states (as noted by John), the gain factor is significantly enhanced at the bandedges[7]. This led Dowling's team to realize that, for an active medium that has dimensions of the order of only a few micrometres, the gain enhancement would be sufficiently large enough to allow low-threshold lasing to occur. This combined research enabled a better understanding of the early work carried out on liquid-crystal lasers and their potential significance. There are a variety of liquid-crystal phases — primarily those containing chiral components — that exhibit a periodic structure and consequently give rise to a photonic bandgap. One of the main advantages of using liquid crystals over photonic crystals is that their periodic structure forms spontaneously, without the need for complex fabrication procedures, and that such soft matter may be readily deformed to achieve facile wavelength tuning.

The first unequivocal observations of bandedge lasing were independently made by Kopp *et al.*[8] and Taheri *et al.*[9,10] in dye-doped chiral nematic liquid crystals. Since then bandedge lasing has subsequently been observed in a variety of different liquid-crystal structures and phases: the chiral smectic phase[11,12], polymeric liquid-crystals[13–17], cholesteric elastomers[18], cholesteric glasses[19,20], an intermediate phase between the chiral nematic phase and the smectic A phase[21], and blue phase I and II[22–24]. In addition, the tuning of bandedge lasing under the influence of external stimuli such as temperature[25–27], ultraviolet illumination[28–30], mechanical stress[17,19] and external electric fields[12,31–34] has also been widely investigated. In many cases fine tuning of the laser wavelength has been demonstrated throughout the visible spectrum. From these collective works it can be seen that the unique optoelectronic properties of liquid crystals give them great potential for use in, and studies of, tunable bandedge lasers. These lasers exhibit the small dimensions of vertical-cavity surface-emitting lasers (VCSELs) but without the need for a sophisticated fabrication procedure, and have the tunability of dye lasers but without relying on the use of toxic liquids.

In addition to lasing at the bandedge, it is also possible to achieve laser emission from a mode situated directly within the photonic bandgap by introducing a defect into the periodic structure[35–40]. In this case the mode is located within the gap, which allows multiple modes to be excited and controlled. This form of lasing, referred to as defect-mode lasing, typically has a lower threshold than that of bandedge lasing and resembles the distributed feedback laser first proposed by Kogelnik and Shank in the early 1970s[41].

Here we aim to present a snapshot of the research carried out so far on laser emission from liquid-crystal media exhibiting periodic structures, focusing in particular on bandedge and defect-mode lasing and on wavelength tuning mechanisms. We will highlight the milestones in emission characteristics that have been reached, and the breakthroughs and innovations that have been made in device architecture. Finally, we will consider the advantages of these lasers over existing technology, the current challenges that lie ahead and the plethora of potential applications.

## Liquid-crystal photonic bandgaps

**Liquid crystals.** Liquid-crystal media represent a class of soft-matter that combines crystalline-like solid ordering with fluid-like behaviour. Liquid crystals are characterized into different mesophases depending on their degree of orientational and positional order[42]. The least-ordered phase is the nematic, which has only long-range orientational order. In this case, the long axes of the molecules point in the same direction (on average), which is

Centre of Molecular Materials for Photonics and Electronics, Electrical Engineering Division, Department of Engineering, Cambridge University, 9 JJ Thomson Avenue, Cambridge CB3 0FA, UK. *e-mail: hjc37@cam.ac.uk



© 2010 Macmillan Publishers Limited. All rights reserved

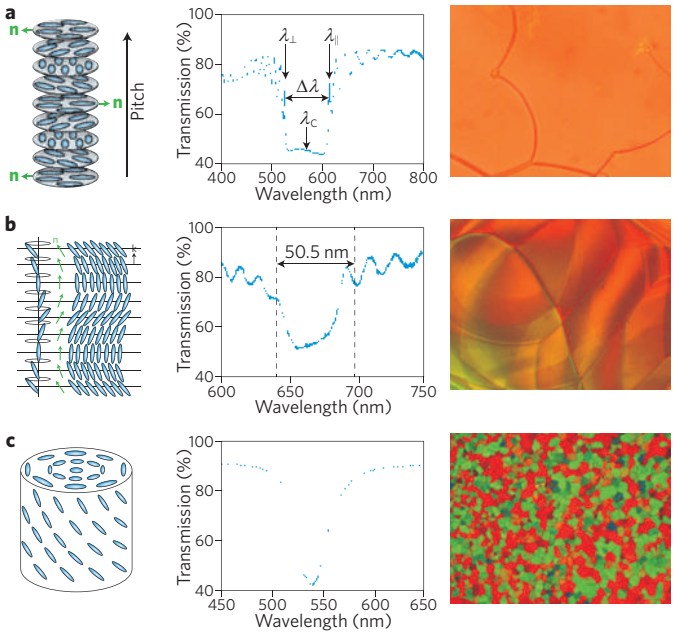


**Figure 1 | Photonic bandgaps for various phases. a**, Chiral nematic. **b**, Chiral smectic. **c**, Blue phase. Figure shows the configuration of the local director for each structure (left), the transmission spectrum for white light (middle) and the corresponding photomicrograph of the optical texture taken when the sample is between crossed polarizers (right) for each of the three phases. In blue phases the double-twist cylinders pack to form a three-dimensional lattice array of defects, with defect lines giving 'Bragg-like' reflections.

defined by a unit vector known as the director, **n**. The macroscopic optical axis lies along the same direction as the director, and it is optically uniaxial[43]. Owing to the microstructure of the phase, many of the macroscopic properties are anisotropic[44,45]. For example, nematic liquid crystals exhibit a birefringence, $\Delta n$, because the refractive index of the extraordinary ray, $n_e$ (often denoted $n_\parallel$ as it is along the director), is different to that of the ordinary ray, $n_o$ (often denoted $n_\perp$ because it is orthogonal to the director), and $\Delta n = n_e - n_o$.

A variant of the nematic phase is the chiral nematic (cholesteric) phase, which spontaneously forms a macroscopic helical structure when either the liquid-crystal molecules are inherently chiral or when chirality is introduced. The presence of chirality causes the director profile to assume a twisted configuration throughout the medium. Figure 1a illustrates rotation of the director about a single axis — the helix axis. In reality, there is no layered structure and the local 'nanoscopic' ordering is identical to that of the nematic phase. The defining length scale of this phase is the pitch — the distance for which the director rotates through an angle of $2\pi$. However, because this phase is also non-polar, the invariance $\mathbf{n} = -\mathbf{n}$ means that the periodicity is only half of the pitch.

Smectic phases are higher-order liquid-crystal phases that combine orientational order with positional order. Unlike the nematic and chiral nematic phases, the density of a smectic phase is not uniform, resulting in a diffuse layered structure. There are a number of different smectic phases, and these are characterized by the packing formation and tilt angle with respect to the layer normal[46]. Each phase is classified by a different letter of the alphabet in the order they were discovered. The least-ordered is the smectic A phase, which has only one-dimensional positional order. Helical smectic phases are also known[47], such as the chiral smectic C* phase, which is similar to the chiral nematic phase except that the molecules are tilted at an angle to the layer normal; it is the precession of the tilt that gives rise to the macroscopic helical structure. Smectic C* liquid crystals, when suitably aligned by surface forces, exhibit ferroelectric properties (Fig. 1b).

More exotic phases known as blue phases (blue phase I, II and III; Fig. 1c)[46–48] have been shown to form laser devices. These are essentially double-twist structures that tend to appear in short-pitch systems between the isotropic and the chiral nematic phases (Fig. 2a). Blue phase I and II exhibit a three-dimensional structure and consequently a three-dimensional photonic bandgap. Until recently the temperature range of these phases was always found to be very small (~2 °C), but now temperature ranges of ~100 °C are achievable through either the artificial process of polymer stabilization[49] or naturally through the use of bimesogenic compounds[50].

**Photonic bandgaps.** Although photonic bandgaps are considered to be a relatively new paradigm, spontaneously forming photonic band structures or one-dimensional Bragg reflectors such as chiral nematic liquid crystals have been in existence for a long period of time. The anisotropic nature of the molecules, combined with the continually rotating director **n**, results in a photonic bandgap when the wavelength of light is comparable to the optical pitch of the helix. This bandgap only exists, however, for circularly polarized light with the same rotation sense as the helix. The same is true for a chiral smectic C* liquid-crystal phase. The bandgap in both cases is therefore considered to be partial and one-dimensional. In contrast, the blue phases I and II exhibit a three-dimensional periodic structure, and therefore an incomplete photonic bandgap exists in each of the three dimensions. The properties of a photonic bandgap in a chiral nematic liquid crystal have been investigated both theoretically and experimentally, with studies ranging from elegant solutions to Maxwell's equations[51–53], which demonstrate the existence of a bandgap, to thermometry devices based on the temperature-induced shift of the reflected colour[1], in what are known as thermochromic liquid crystals.

Example transmission spectrums for a chiral nematic, a chiral smectic C* and blue phase I are shown in Fig. 1, along with a schematic of the molecular configuration for each phase and a photomicrograph of the optical texture observed for white-light transmittance through crossed polarizers. The fundamental wavelengths that describe each bandgap are indicated. At each local maximum either side of the bandgap, a resonant (localized) potential lasing mode exists. In the examples shown, the wavelength output at the short and long bandedges corresponds to the first maximum in the transmission oscillations on either side of the photonic bandgap, the edges of which are denoted by $\lambda_\perp$ and $\lambda_\parallel$ and the centre of which is denoted by $\lambda_C$.

## Bandedge lasers

**Creating a bandedge liquid-crystal laser.** Two primary factors are important for bandedge laser emission to occur in liquid-crystal media. First, a light harvester of some form must be present. This can be either a rare-earth element or a laser dye such as DCM or PM597. The dye can either be dispersed into the liquid-crystal matrix or it can form a subunit of the liquid-crystalline molecule. Ultraviolet lasing has been observed from purely liquid-crystal samples without the addition of a dye[54]. The second factor is the spectral position of the photonic bandgap relative to the emission spectrum of the light emitter. To achieve laser action, one edge of the photonic bandgap must overlap the emission spectrum, and these must be matched to maximize coupling efficiency and thus achieve the lowest possible threshold. The short- and long-wavelength bandedges are not equivalent for liquid crystals, and this is because the alignment of the electric field vector of the propagating mode at the specific bandedge is different to that of the transition dipole moment of the dye[55]. For the majority of the studies carried out so far, the



© 2010 Macmillan Publishers Limited. All rights reserved

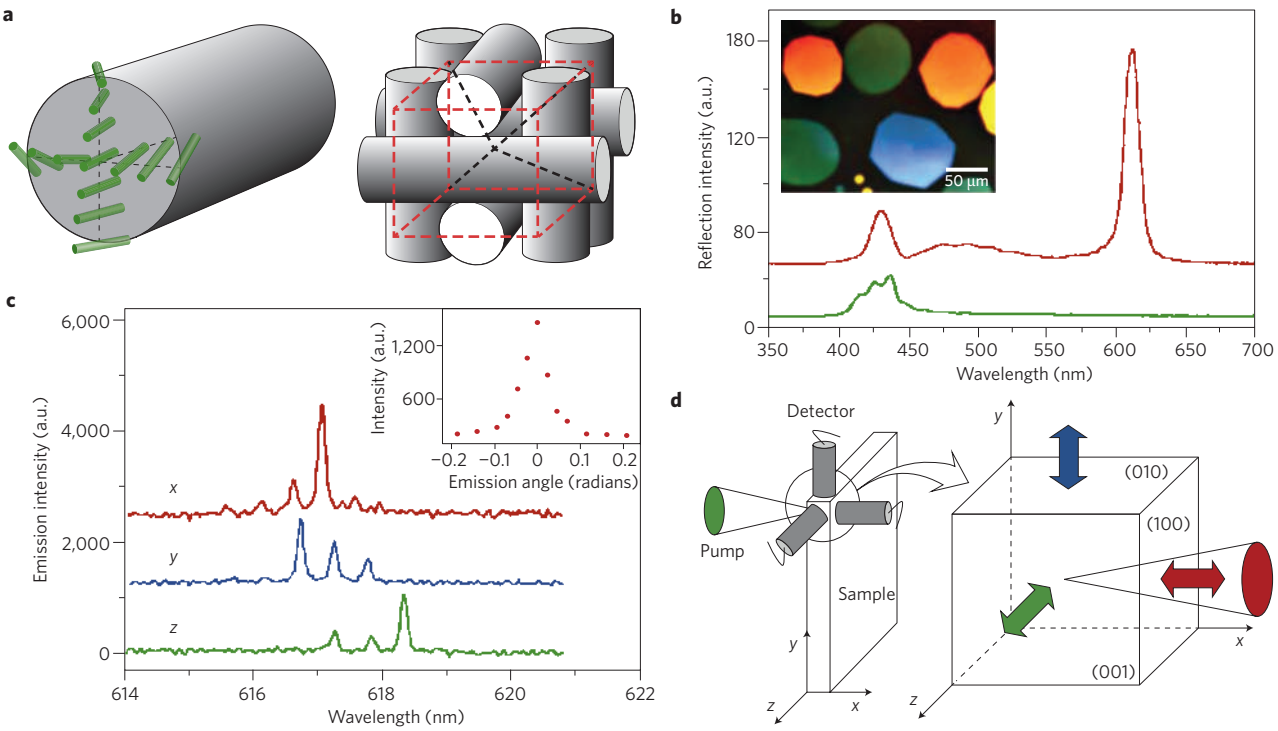


**Figure 2 | Laser emission in three dimensions from a blue phase II liquid crystal. a**, Illustration of the double-twist structure. **b**, Reflection spectrum for a particular platelet (shown inset). **c**, Emission spectrum in the three orthogonal directions. **d**, Region of the sample from which the emission was recorded. Figure reproduced with permission from ref. 22, © 2002 NPG.

long-wavelength bandedge has proved to be the lowest threshold mode because the transition dipole moment of the dye and the electric field vector are more collinear than they are perpendicular to one another.

Laser emission from liquid-crystal structures is generally achieved through optical pumping, using either picosecond or nanosecond pulses from solid-state lasers such as Nd:YAG. Increasing the pulse width from picoseconds to nanoseconds was found to increase the excitation threshold[56] (in units of energy per unit area per pulse) in accordance with two-level laser theory. The repetition rate must also be chosen carefully, as observed in ref. 57. The wavelength-dependence of the dye absorption defines the excitation wavelength. However, it has been shown[58] that shorter excitation wavelengths below the absorption maximum result in a lower threshold, and this may be related to the overlap between the Beer–Lambert-like dependence of absorption through the cell and the spatial dependence of the modal electric field vector[59].

In terms of the geometry for optical pumping, liquid-crystal lasers can be photopumped from any angle but will always emit along the direction defined by the helix axis. It has been shown, however, that for incident angles greater than 18° the emission intensity of liquid-crystal lasers depends significantly on their incident polarization[60], and careful consideration is therefore devoted to selecting the correct polarization when pumping at oblique incidence. It has also been shown theoretically[61], and with some experimental verification[62], that the threshold can be reduced using an excitation beam with the same polarization handedness as the rotation sense of the helix, and at the shorter-wavelength bandedge so as to increase the density of states. This has been achieved using a layered, randomly amplifying medium[63]. Other forms of optical excitation that have been reported include two-photon pumping[64] and two liquid-crystal lasers[65] in tandem.

The most common phase used for liquid-crystal lasers is the chiral nematic, because it is easily formed from nematic compounds using chiral dopants and has a broad temperature range. Although chiral smectic phases have also been used for liquid-crystal lasers, their benefits over the chiral nematic phase for such applications are not yet clear (apart from their ferroelectric coupling to applied electric fields, which is very useful for wavelength tuning). Blue phases, however, do have considerable benefits over their chiral nematic counterparts, but achieving laser emission from such structures is non-trivial. One major benefit is that laser emission in three orthogonal directions can be obtained simultaneously by virtue of the three-dimensional photonic bandgap. This was first demonstrated using blue phase II, which exhibits a double-twist structure (Fig. 2)[22]. Laser emission has also been demonstrated from both a polymer-stabilized blue phase I[23] and a wide-temperature blue phase I[24] (Fig. 3). For the wide-temperature blue phase I, the excitation threshold energy was found to be lower than that of a corresponding chiral nematic liquid crystal under similar experimental conditions (that is, dye and liquid-crystal structures, dye concentration, position of bandedge, sample thickness and similar excitation).

Bandedge laser emission has also been observed from holographic polymer-dispersed liquid-crystal (H-PDLC) lasers, which, unlike other aforementioned devices, do not form naturally and thus require some form of fabrication procedure. These H-PDLCs are liquid-crystal droplets — usually either a nematic or chiral nematic — dispersed within a polymer matrix formed using a photocuring technique. Although the linewidths that have been achieved so far are typically higher than those measured for conventional low-molar-mass liquid-crystal bandedge lasers, H-PDLCs do offer advantages in terms of tuning the laser wavelength and forming two-dimensionally patterned structures[66–70]. Both reflection[67] and transmission gratings[68] have so far been studied, although transmission gratings seem to exhibit more efficient laser emission and have lower thresholds than reflection gratings.



© 2010 Macmillan Publishers Limited. All rights reserved

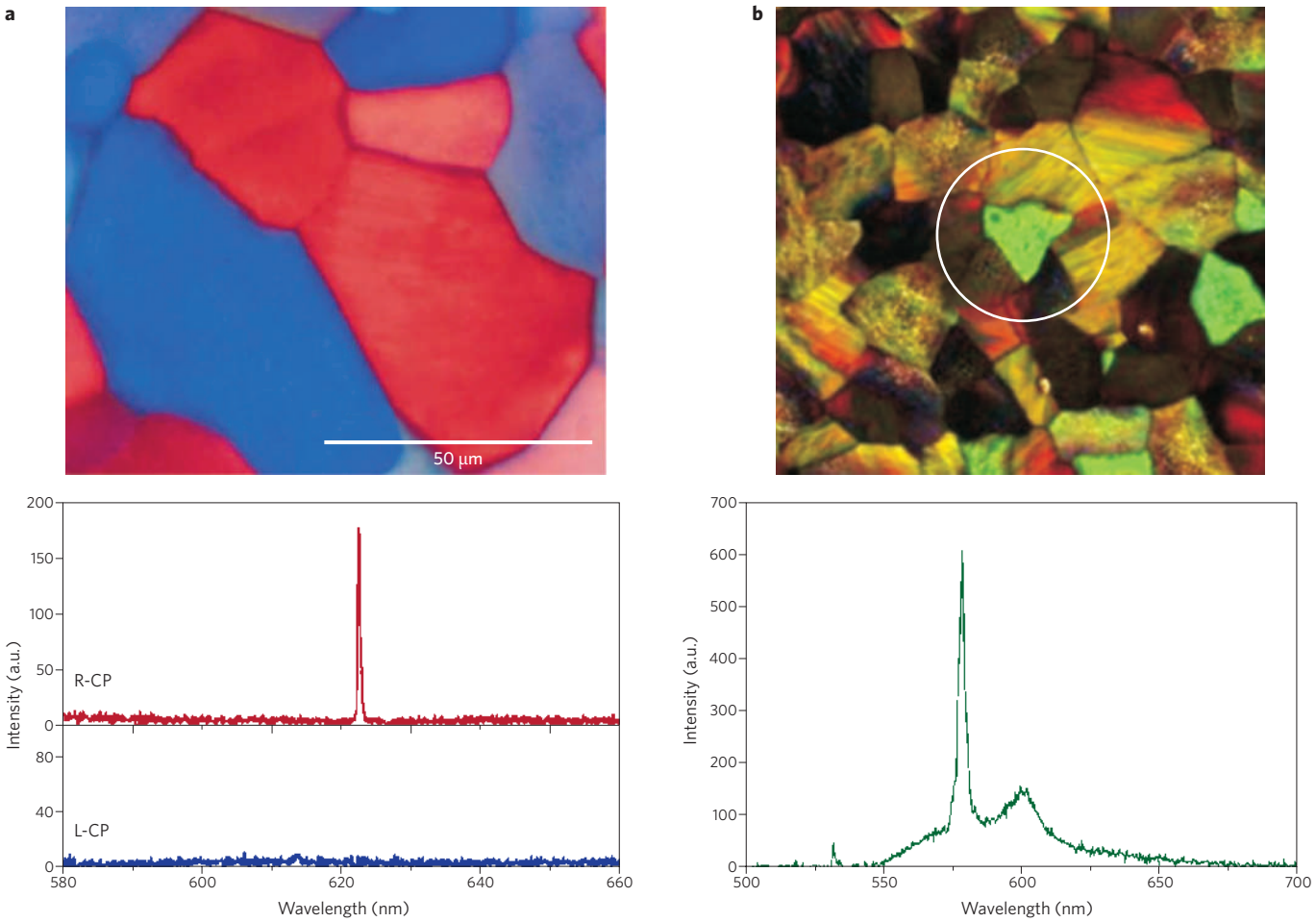


**Figure 3 | Low-threshold laser emission from blue phase I. a**,**b**, Platelet structure (top) and emission spectrum (bottom) for a polymer-stabilized blue phase (**a**) and a wide-temperature blue phase (**b**). R-CP and L-CP denote right- and left-circularly polarized light, and the white circle in **b** indicates the lasing blue phase platelet. Figure reproduced with permission from: **a**, ref. 23, © 2006 Wiley; **b**, ref. 24, © 2006 SID.

There have also been demonstrations of laser emission from liquid crystals that do not naturally form periodic structures. For example, it has been shown that laser emission can occur from a device comprising a plane layer of dye-doped nematic liquid crystal sandwiched between one substrate with a uniform transparent indium tin oxide layer and a second substrate that consists of periodic and parallel chromium electrodes. Periodic modulation of the gain in the medium can be achieved because the chromium electrodes are non-transparent. Applying an electric field modulates the refractive index due to the reorientation of the nematic director in regions above the chromium electrodes, thus creating a Bragg resonator structure[71,72]. Laser emission has also been observed from a dye-doped nematic phase without any modulation in the refractive index or gain medium using a plane waveguide geometry[73].

**General emission characteristics.** General laser emission characteristics for a bandedge liquid-crystal laser are shown in Fig. 4. A typical laser emission spectrum at the edge of a chiral nematic bandgap, when photopumped with 5 ns pulses from a *Q*-switched Nd:YAG laser of wavelength 532 nm, is shown in Fig. 4a. 532 nm falls within the wavelength range of the absorption spectrum of many laser dyes, including DCM, which has been extensively used in liquid-crystal lasers. Emission is bidirectional along the helix axis. The sample was a commercial nematic liquid-crystal mixture doped with a chiral additive and DCM dye, housed in a 7.5-μm-thick planar aligned glass cell and operated at a temperature of 30 °C.

Figure 4a shows emission relative to the bandgap, with the transmission spectrum for white light plotted on the left-hand vertical axis and the laser emission spectrum presented on the right-hand vertical axis. Here, the spectrometer has captured the long-wavelength part of the photonic bandgap — the flat region of 590–603 nm — as well as the maxima and minima of four subsidiary oscillations. The emission intensity of the laser line was found to peak at 604.65 nm, which is located at a slightly longer wavelength than the transmission maximum ($\lambda_e$ = 604.36 nm). This offset is to be expected because the laser mode is not positioned at the bandedge in finite-thickness samples. It is also shown in this example that the linewidth of the laser line is 0.13 nm. This yields a *Q*-factor of the laser mode ($Q = \lambda_r/\Delta\lambda$) of ~4,600. From this a rough estimate of the coherence length, $\xi_{coh}$, using the linewidth ($\xi_{coh} = \lambda_r^2/\Delta\lambda_r$) was found to be ~5 mm.

It has been shown[74] that the emission from a liquid-crystal bandedge laser can exhibit a large coherence area. This offers a potential means of removing heat from the system, opening up the possibility for large output powers and thus increasing the laser dye lifetime. Figure 4b is an example of the far-field spot of a bandedge liquid-crystal laser, showing central and subsidiary maxima. The output of such a laser is near-Gaussian (Fig. 4c,d). However, despite the multitude of reports on bandedge lasing so far, there have been no reports dedicated to the measurement of



© 2010 Macmillan Publishers Limited. All rights reserved

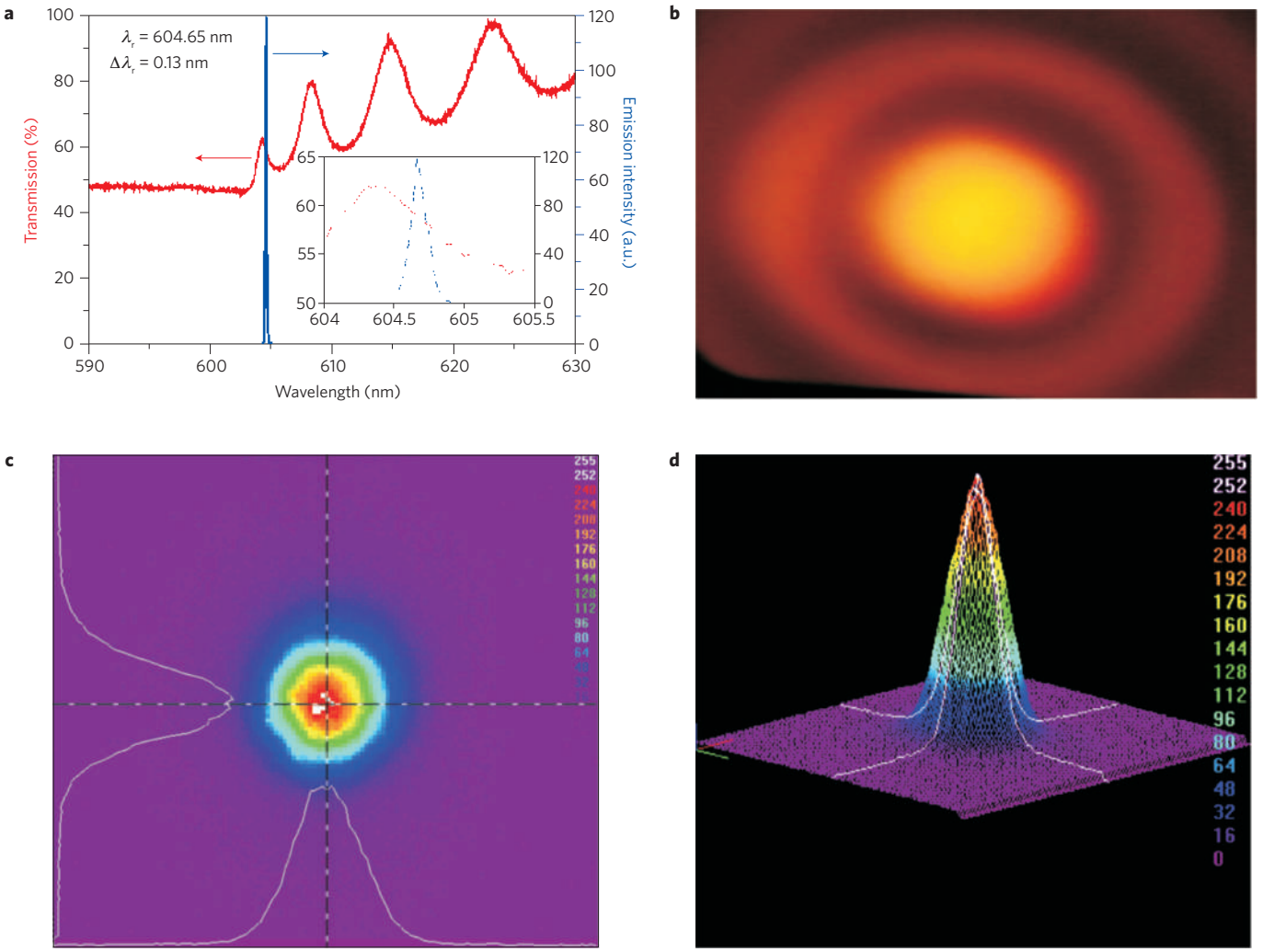


**Figure 4 | Typical emission characteristics of a bandedge liquid-crystal laser. a**, The emission spectrum plotted relative to the long-wavelength photonic bandedge, where the inset shows a zoomed image of the transmission spectrum and laser emission close to the first minimum of the transmission spectrum. **b**, Far-field laser spot. **c**, Energy profile of the laser in the far-field in two dimensions. **d**, Energy profile of the laser in the far-field in three dimensions. The scales in **c** and **d** show energy intensity, in arbitrary units, in the range of 0–255. Figure reproduced with permission from: **a**,**b**, ref. 24, © 2006 SID; **c**,**d**, ref. 121, © 2006 Elsevier.

the coherence length of a bandedge liquid-crystal laser. A colour-cone angle laser was recently demonstrated[75]. The axial output of a bandedge liquid-crystal laser is usually circularly polarized, although an aluminium mirror can be used to achieve linearly polarized emission[76].

**Performance-related properties.** The two important parameters used to characterize a liquid-crystal laser are the excitation threshold and the slope efficiency, and research has shown that these are influenced by a number of liquid-crystal-related parameters. These parameters include, but are not limited to, the birefringence of the medium[77–79] (a factor that is also shown to be important in the bandedge lasing of photonic crystals), the orientational order parameter[19,77,78] and the order parameter of the transition dipole moment of the dye[80–82]. Polymeric dyes were used to achieve good alignment between the liquid crystal and the transition dipole moment, resulting in a high order parameter[80]. Oligofluorene dyes have been shown to exhibit very high order parameters and high quantum yields[83] in a liquid-crystal host, which generally results in better laser efficiency[81,82]. Other high-quantum-yield dyes recently used include pyrenes[84], which can decrease the excitation threshold by an order of magnitude compared with DCM and PM597, which can increase slope efficiencies to over 30%[85]. These materials cause a drop in laser threshold due to the significant overlap of the electric field vector of the optical eigenmode with the dye's transition dipole moment[55]. Recent research suggests that by maximizing key metrics such as order parameters, birefringence and dye quantum yields, the threshold can be reduced and the slope efficiency increased. Typical values of slope efficiency reported are often greater than 30%[24] — a value comparable to that of conventional liquid dye lasers — and may reach as high as 70%[86].

Improving these materials factors alone may not be sufficient to reduce the threshold such that a low-power incoherent input source, such as an electroluminescent layer or a light-emitting diode, can be used. Additionally, innovations in the device structure that ensure optimum photon confinement are likely to be essential for further improvement. For example, emission intensities have been increased by a factor of eight using a stack of multiple dye-doped chiral polymer films[87], and have also been increased using a mirror or chiral nematic liquid-crystal polymer film to ensure that emission along the helix occurs only in one direction[88,89]. Polymer stabilization and cholesteric glasses have also been shown to improve the emission intensity by reducing thermal fluctuations and thus increasing the order parameter[19,20].



© 2010 Macmillan Publishers Limited. All rights reserved

Mechanically flexible and rugged bandedge lasers have also been demonstrated by forming polymerized free-standing films based on photopolymerized chiral nematic liquid crystals[17–19]. Even in the presence of mechanical distortion the film still maintains a laser output. The polymerization process also provides a secondary benefit in that it removes any temperature dependence of the helical pitch. As a result, the laser wavelength remains constant over a wide temperature range.

The use of a planar amplifier based on a dye-doped isotropic layer has been shown to achieve a sevenfold improvement in output for a 4-mm-thick chiral nematic laser system[90]. Using a dye-doped nematic layer has also proven to be beneficial and, owing to the layer anisotropy, the amplification coefficient was observed to be anisotropic[91]. Quasi-in-plane leaky modes, formed as a result of Fresnel reflections from the glass substrates, can lead to optical losses that take energy away from the normal Bragg modes along the helix axis[92,93], but lateral confinement[94] may provide a solution to this.

**Laser arrays.** Inorganic VCSELs made significant progress with the introduction of laser arrays, which enabled higher output powers to be obtained from a single device by coupling the output from each emitter in the array matrix. If the emitters are in-phase then the output power scales as $N^2$, where $N$ is the number of elements in the laser array. Similar arrays have also been formed using liquid crystals to decrease the threshold by exploiting the Purcell effect, and are used to generate polychromatic laser emission for displays[69,94–96]. Examples of such laser arrays are shown in Fig. 5, which includes the 'polycrips' structure (Fig. 5a)[94] and a patterned dye-doped reflective H-PDLC with alternating pitch lengths (Fig. 5b)[69]. Figure 5c shows simultaneous red–green–blue emission generated from a conventional liquid-crystal cell using a microlens array to redistribute the pump so as to generate multiple gain regions[96]. Single pixels of this laser have been driven to give quasi-continuous-wave output powers of 5 mW at 3 kHz, which, when combined in the far-field, give a potential output of several watts[86].

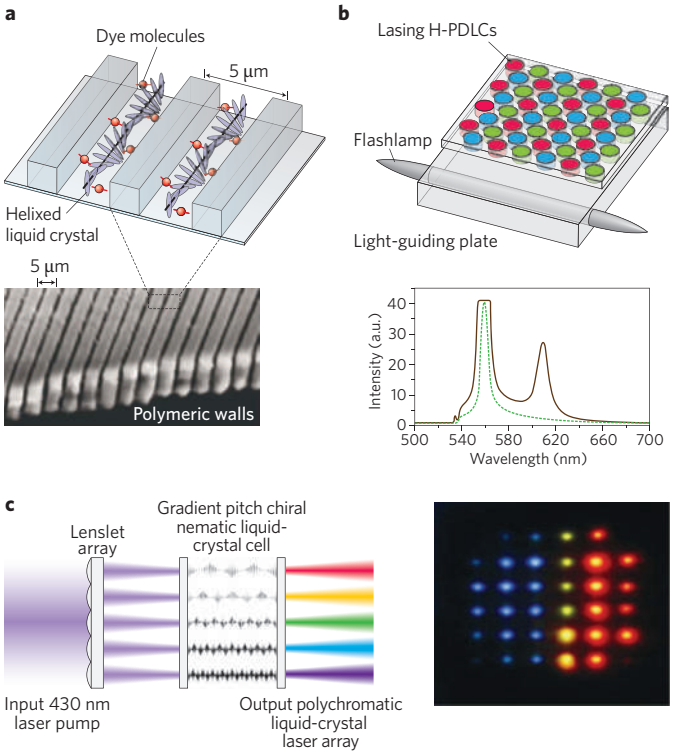


**Figure 5 | Liquid-crystal laser arrays. a**, The 'polycrips' structure developed at the University of Calabria. **b**, A patterned two-dimensional H-PDLC array containing three different pitches. **c**, Two-dimensional array using a microlens array to create an array of active gain regions (left) and the resulting simultaneous red–green–blue output (right). Figure reproduced with permission from: **a**, ref. 94, © APS 2005; **b**, ref. 69, © 2007 SID; **c**, ref. 96, © 2008 OSA.

## Defect-mode lasers

Defect-mode lasers differ from bandedge lasers in that a resonant channel exists within the photonic bandgap itself, thus confining the energy to this mode. Hence, because of the bandgap, there is no spontaneous emission either side of the laser mode; that is, the mode is localized at the defect. This is analogous to the distributed feedback lasers that Kogelnik and Shank studied in the 1970s[41], which have now become widespread in semiconductor laser technology. There are a number of ways of creating a defect-mode laser, ranging from introducing a 90° phase slip in the periodicity of the helical structure to inserting a thin layer of isotropic liquid or nematic liquid crystal between chiral nematic liquid-crystal mirrors (Fig. 6).

**Structures for defect-mode lasing.** Defect-mode liquid-crystal structures have been studied both theoretically[35–37,97] and experimentally[98–103], and a number of different approaches for creating a defect have been suggested. Early research focused on introducing a phase jump[36,38] or an isotropic layer[35,38,98] into the chiral nematic material. The phase jump, induced by twisting one part of the helical structure, creates a single localized mode that is circularly polarized and corresponds to a peak in the transmission. The use of an isotropic layer sandwiched between chiral nematic layers is analogous to VCSELs consisting of an amplifying defect layer between periodic dielectric 'mirrors', which has shown to result in ultralow-threshold lasing. Defect-mode lasers later progressed to architectures involving dye-doped nematic polymer layers sandwiched between conventional chiral nematic liquid-crystal polymer layers[39,99–102]. This resulted in the emergence of a new form of defect-mode lasing related to phase retardation through an inserted anisotropic layer. Although the defect layer was typically thin, thick layers (100 μm) inserted between thin chiral nematic polymer layers (similar to a conventional laser cavity between mirrors) have also been studied, yielding multimode emission due to the multiple resonant states situated within the bandgap[99].

Different incarnations of defect-mode structures involving cholesteric layers of various pitches have also been reported, leading to electrotunable non-reciprocal laser emission, and a left-handed cholesteric structure between right-handed chiral nematics. Two-layered heterostructures consisting of right- and left-handed chiral nematics have also been demonstrated[100–102]. It was shown that three-layer heterostructures have a significantly lower threshold than single- and two-layer devices. This results from a much larger density of photon states and a high-$Q$-factor cavity. For structures consisting of a chiral nematic defect sandwiched between two thicker layers of the same handedness, the excitation threshold can be further reduced when the defect-mode coincides with the bandedge. Innovative structures based on Fibonaccian sequences, which are well-studied in quasi-crystals, have also been translated to liquid crystals in the form of a stack of single-pitched chiral nematic layers simultaneously exhibiting multiple bandgaps from a single device. Multiwavelength laser emission has also been demonstrated from multiple-photonic-bandgap structures[104,105].

Defect-mode lasers have attracted a great deal of interest because of the wide variety of configurations available, with each one providing a means of increasing the density of photon states and altering the number of resonant modes available within the



© 2010 Macmillan Publishers Limited. All rights reserved

bandgap. Furthermore, their high density of states means that a defect-mode laser typically has a lower excitation threshold than that of a corresponding bandedge laser. However, because the mode is pinned to the defect, the maximum emission energy that can be obtained is lower than that of a bandedge laser, and thus a trade-off between emission energy and threshold must be made.

## Tunability

A large proportion of the research carried out so far has focused on wavelength tuning liquid-crystal lasers using a variety of different external stimuli, and it is this sensitivity that makes them particularly attractive as laser sources. External stimuli that have been used for wavelength tuning include temperature, ultraviolet illumination, mechanical stress, spatial variation and electric field.

**Mechanically induced tuning.** Mechanical tuning has been reported for cholesteric elastomers stretched laterally to contract the pitch. Biaxial stretching of the elastomers gave a corresponding change in pitch of up to 150 nm, resulting in a change in laser wavelength from ~540 nm to 630 nm (ref. 18). Large shifts (~80 nm) in laser wavelength have also been recently observed on biaxial stretching of a chiral nematic polymer film[16].

**Thermally induced tuning.** Thermally induced changes in the helical pitch can be used to vary the emission wavelength of a liquid-crystal laser[25–27]. An increase in helical pitch causes the wavelength to red-shift, whereas a decrease causes a blue-shift. The laser wavelength varies in a stepwise manner because pitch changes in a chiral nematic liquid crystal are discrete with temperature for thin films. These discontinuities in the laser wavelength can be removed by adding two chiral dopants with opposing temperature dependencies on the helical twisting power[106].

**Spatial tuning.** Spatial tuning has been discussed in several reports[107–114] and typically involves forming a pitch gradient, together with a variety of dyes, to cover a wide proportion of the visible spectrum. Wavelength tuning is achieved by varying the position of the cell relative to the pump beam. Wideband emission has been demonstrated using a sample containing a number of different dyes and a pitch gradient[107]. In this case, six different dyes were dispersed into a chiral nematic liquid-crystal sample. Some of the dyes acted as Forster transfer elements by decoupling excitation and emission processes. Laser emission from a single cell was tuned from ~350 nm to 700 nm. Spatial tuning has also been observed in photopolymerized chiral nematic polymer films, in which the pitch gradient has been 'frozen-in' due to the formation of the polymer network[110]. Polymerization of the structure is particularly important for prolonging the lifetime of the laser by preventing unwanted chiral dopant and dye diffusion. This also ensures that the same area of the sample produces the same laser emission wavelength.

More than one dye is required for spatial tuning, and indeed many other forms of tuning that cover a broad wavelength range. To excite all the dyes at a single fixed wavelength, despite the fact that the absorption bands of the dyes may not overlap, Forster transfer is a particularly useful mechanism in these situations[115] and has been shown to reduce the excitation threshold in some cases[116].

**Photochromic tuning.** Dispersing photoactive agents into the liquid-crystal matrix makes it possible to adjust the periodicity of the chiral structure by irradiating the sample with ultraviolet light[28–30,117,118]. Reports have shown that wideband wavelength tuning (610–700 nm) can be achieved by adjusting the exposure energy of the ultraviolet light source[29]. Phototunability has also been achieved by varying exposure time instead of exposure energy[28]. An increase in tuning range has also been achieved by using two different dyes, DCM and PM580, dissolved in a liquid crystal host. However, this approach has the unfortunate drawback of being irreversible in most cases. Reversibility can be achieved using photochromic compounds such as sugar derivatives with plural azobenzene substituents, in which the *trans–cis* and *cis–trans* conformation changes can be induced using ultraviolet and visible light, respectively. Reversible tuning has also been demonstrated through photoisomerization of novel chiral azo dyes[28]. In this study, the helical pitch changed during ultraviolet illumination (with a corresponding blue-shift of approximately 15 nm) but returned to its undistorted state when the illumination was removed. Similar optical tuning has been reported in defect-mode lasers through a *cis–trans* conformation change, resulting in a contraction of the pitch in the defect layer relative to that of the other two layers[40].

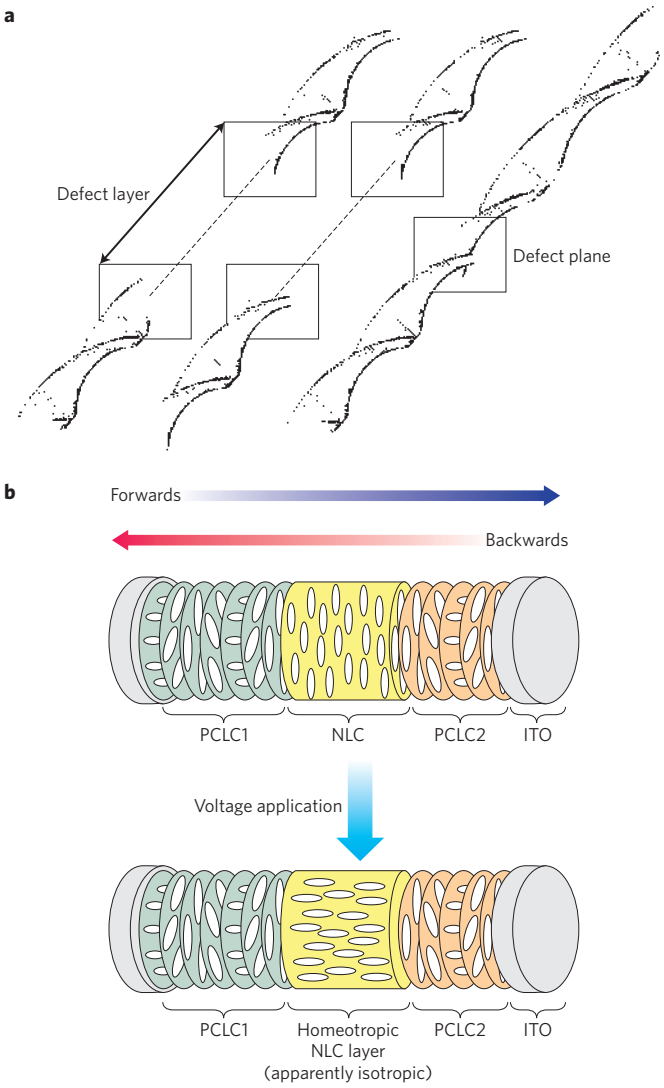


**Figure 6 | Defect-mode liquid-crystal structures. a**, A defect is introduced through a phase jump in the helical structure. **b**, The defect is a nematic liquid-crystal laser, where PCLC and NLC refer to polymer and nematic liquid crystals, respectively, ITO refers to the indium tin oxide electrodes, and the forwards and backwards arrows show the direction of the incident pump laser. Figure reproduced with permission from: **a**, ref. 37, © 2003 EDP; **b**, ref. 101, © 2006 Wiley.

**Electric-field tuning.** The response of liquid crystals to an electric field provides numerous ways in which wavelength tuning



© 2010 Macmillan Publishers Limited. All rights reserved

can be achieved. For bandedge lasers, different geometries and coupling mechanisms have been exploited to alter the pitch of the structure[12,31–34]. The pitch can either be unwound, as shown[32] for a chiral smectic liquid crystal using ferroelectric coupling[32] and for a chiral nematic liquid crystal with a positive dielectric anisotropy using in-plane electrodes[24,34], or contracted using chiral nematics with a negative dielectric anisotropy[33].

Directly addressing the defect layer of a defect-mode laser using an electric field has also been shown to achieve wavelength tuning[101]. An example of this is to adjust the effective refractive index of the layer by reorienting the nematic director in the defect. Altering the pitch of the ferroelectric liquid-crystal layer sandwiched between dielectric mirrors was also found to change the laser wavelength[32]. Voltage-controlled lasing has also been demonstrated, both in terms of intensity and emission spectrum, for a configuration consisting of a nematic liquid crystal sandwiched between two chiral nematic layers[119].

## Applications

In principle, there are numerous technologies that liquid-crystal lasers could be applied to. Such lasers could even replace semiconductor VCSELs in many respects if the present challenges are overcome. Perhaps the most obvious application is a laser-based display; reports have already shown that it is possible to produce red–green–blue laser emission simultaneously and, given their high spectral purity and micrometre-sized cavity length, liquid-crystal lasers could provide the necessary elements to produce a large-area projection display without colour filters or polarizers and a colour gamut and at a resolution that outperforms current state-of-the-art lamp projectors. The capability of these lasers to be tunable and fabricated as a single flexible substrate also opens up the possibility for 'friend or foe' identification, in which a specifically encoded emitted wavelength could be used to indentify a 'friend', as opposed to an unknown 'foe', when emitting a narrow-linewidth laser pulse under optical excitation. Given the broad range of wavelengths that are achievable for a single sample, such lasers could be used for spectroscopy, medical diagnostics and skin treatments requiring a range of different wavelengths for various penetration depths. Infrared lasers are of interest for non-invasive point-of-care treatments, such as for the optical removal of blood clots. Liquid-crystal lasers are advantageous here because they are compact, simple to construct and can emit multiple wavelengths when excited by a single excitation wavelength. This would avoid the multiple bulky laser sources currently required for many spectroscopic and medical applications.

## Objectives and challenges

The ultimate aim is to achieve pumping using low-power incoherent optical excitation. At present, pumping is restricted to high-intensity optical pulses of short duration, although stimulated emission has been demonstrated at visible wavelengths using blue light-emitting diodes. However, the threshold for lasing must be further reduced before a low-power incoherent light source can be used. Studies are currently being carried out[120] to develop low-threshold lasers that could, in principle, be driven with an electroluminescent layer, an inorganic or organic light-emitting diode or light-emitting polymer. We must not understate the prospect of an all-organic device that is compact (millimetre thickness), wavelength-tunable and quasi-continuous-wave. This Review has highlighted the significant steps that have already been taken towards this goal, but these properties have yet to be demonstrated simultaneously in a single device.

## References


1. Yang, D.-K. & Wu, S.-T. *Fundamentals of Liquid Crystal Devices* (Wiley, 2006).
2. Reinitzer, F. Beiträge zur Kenntniss des Cholesterins. *Monatsh. Chem.* **9,** 421–441 (1888).
3. Il'chishin, I., Tikhonov, E., Tishchenko, V. & Shpak, M. Generation of a tunable radiation by impurity cholesteric liquid crystals. *JETP Lett.* **32,** 24–27 (1978).
4. Goldberg, L. S. & Schnur, J. M. Tunable internal-feedback liquid crystal-dye laser. US patent 3,771,065 (1973).
5. Yablonovitch, E. Inhibited spontaneous emission in solid state physics and electronics. *Phys. Rev. Lett.* **58,** 2059–2062 (1987).
6. John, S. Strong localization of photons in certain disordered dielectric superlattices. *Phys. Rev. Lett.* **58,** 2486–2489 (1987).
7. Dowling, J. P., Scalora, M., Bloemer, M. J. & Bowden, C. M. The photonic band-edge laser: A new approach to gain enhancement. *J. Appl. Phys.* **75,** 1896–1899 (1994).
8. Kopp, V. I., Fan, B., Vithana, H. K. M. & Genack, A. Z. Low-threshold lasing at the edge of a photonic stop band in cholesteric liquid crystals. *Opt. Lett.* **23,** 1707–1709 (1998).
9. Taheri, B., Munoz, A., Palffy-Muhoray P. & Twieg, R. Low threshold lasing in cholesteric liquid crystals. *Mol. Cryst. Liq. Cryst.* **358,** 73–82 (2001).
10. Alvarez, E. *et al.* Mirrorless lasing and energy transfer in cholesteric liquid crystals doped with dyes. *Mol. Cryst. Liq. Cryst.* **369,** 75–82 (2001).
11. Ozaki, M., Kasano, M., Ganzke, D., Hasse, W. & Yoshino. K. Mirrorless lasing in a dye-doped ferroelectric liquid crystal. *Adv. Mater.* **14,** 306–309 (2002).
12. Ford, A. D., Morris, S. M., Pivnenko, M. N. & Coles, H. J. A comparison of photonic band edge lasing in the chiral nematic N* and smectic C* phases. *Proc. SPIE* **5289,** 213–220 (2004).
13. Schmidtke, J., Stille, W., Finkelmann, H. & Kim, S. T. Laser emission in a dye doped cholesteric polymer network. *Adv. Mater.* **14,** 746–749 (2002).
14. Shibaev, P. V., Tang, K., Genack, A. Z., Kopp, V. & Green, M. M. Lasing from a stiff chain polymeric lyotropic liquid crystal. *Macromolecules* **35,** 3022–3025 (2002).
15. Matsui, T., Ozaki, R., Funamoto, K., Ozaki, M. & Yoshino, K. Flexible mirrorless laser based on a free-standing film of photopolymerized cholesteric liquid crystal. *Appl. Phys. Lett.* **81,** 3741–3743 (2002).
16. Shibaev, P. V., Madsen, J. & Genack, A. Z. Lasing and narrowing of spontaneous emission from responsive cholesteric films. *Chem. Mater.* **16,** 1397–1399 (2004).
17. Ohta, T. *et al.* Monodomain film formation and lasing in dye-doped polymer cholesteric liquid crystals. *Jpn. J. Appl. Phys.* **43,** 6142–6144 (2004).
18. Finkelmann, H., Kim, S. T., Muñoz, A., Palffy-Muhoray, P. & Taheri, B. Tunable mirrorless lasing in cholesteric liquid crystalline elastomers. *Adv. Mater.* **13,** 1069–1072 (2001).
19. Shibaev, P. V., Kopp V., Genack, A. & Hanelt, E. Lasing from chiral photonic band gap materials based on cholesteric glasses. *Liq. Cryst.* **30,** 1391–1400 (2003).
20. Wei, S. K. H., Chen, S. H., Dolgaleva, K., Lukishova, S. G. & Boyd R. W. Robust organic lasers comprising glassy-cholesteric pentafluorene doped with a red-emitting oligofluorene. *Appl. Phys. Lett.* **94,** 041111 (2009).
21. Chanishvili, A. *et al.* Lasing in an intermediated twisted phase between cholesteric and smectic A phase. *Appl. Phys. Lett.* **88,** 101105 (2006).
22. Cao, W., Muñoz, A., Palffy-Muhoray, P. & Taheri, B. Lasing in a three-dimensional photonic crystal of the liquid crystalline blue phase II. *Nature Mater.* **1,** 111–113 (2002).
23. Yokoyama, S., Mashiko, S., Kikuchi, H., Uchida, K. & Nagamura, T. Laser emission from a polymer-stabilized liquid-crystalline blue phase. *Adv. Mater.* **18,** 48–51 (2006).
24. Morris, S. M. *et al.* The emission characteristics of liquid crystal lasers. *J. Soc. Inf. Display* **14,** 565–573 (2006).
25. Funamoto, K., Ozaki, M. & Yoshino, K. Discontinuous shift of lasing wavelength with temperature in cholesteric liquid crystal. *Jpn. J. Appl. Phys.* **42,** L1523–L1525 (2003).
26. Morris, S. M., Ford, A. D., Pivnenko, M. N. & Coles, H. J. Enhanced emission from liquid-crystal lasers. *J. Appl. Phys* **97,** 023103 (2005).
27. Huang, Y., Zhou, Y., Doyle, C. & Wu, S.-T. Tuning the photonic band gap in cholesteric liquid crystals by temperature-dependent dopant solubility. *Opt. Express* **14,** 1236–1242 (2006).
28. Chanishvili, A. *et al.* Phototunable lasing in dye-doped cholesteric liquid crystals. *Appl. Phys. Lett.* **8,** 5353–5355 (2003).
29. Furumi, S., Yokoyama, S., Otomo, A. & Mashiko, S. Phototunable photonic bandgap in a chiral liquid crystal laser device. *Appl. Phys. Lett.* **84,** 2491–2493 (2004).
30. Shibaev, P. V., Sanford, R. L., Chiappetta, D., Milner, V. & Genack A. Z. Light controllable tuning and switching of lasing in chiral liquid crystals. *Opt.Express* **13,** 2358–2363 (2005).
31. Furumi, S., Yokoyama, S., Otomo, A. & Mashiko, S. Electrical control of the structure and lasing in chiral photonic band-gap liquid crystals. *Appl. Phys. Lett.* **82,** 16–18 (2003).




© 2010 Macmillan Publishers Limited. All rights reserved

32. Kasano, M., Ozaki, M., Yoshino, K., Ganzke, D. & Haase, W. Electrically tunable waveguide laser based on ferroelectric liquid crystals. *Appl. Phys. Lett.* **82,** 4026–4028 (2003).
33. Lin, T.-H. *et al.* Electrically controllable laser based on cholesteric liquid crystal with negative dielectric anisotropy. *Appl. Phys. Lett.* **88,** 061122 (2006).
34. Woltman, S. J. & Crawford, G. P. Tunable cholesteric liquid crystals lasers through in-plane switching. *Proc. SPIE* **6487,** 64870B (2007).
35. Yang, Y.-C. *et al.* Photonic defect modes of cholesteric liquid crystals. *Phys. Rev. E.* **60,** 6852–6854 (1999).
36. Kopp, V. I. & Genack, A. Z. Twist defect in chiral photonic structures. *Phys. Rev. Lett.* **89,** 033901 (2002).
37. Schmidtke, J. & Stille, W. Photonic defect modes in cholesteric liquid crystal films. *Eur. Phys. J. E* **12,** 553–564 (2003).
38. Schmidtke, J., Stille, W. & Finkelmann, H. Defect mode emission of a dye doped cholesteric polymer network. *Phys. Rev. Lett.* **90**, 083902 (2003).
39. Song, M. H. *et al.* Effect of phase retardation on defect-mode lasing in polymeric cholesteric liquid crystals. *Adv. Mater.* **16,** 779–783 (2004).
40. Matsui, T., Ozaki, M. & Yoshino, K. Tunable photonic defect modes in a cholesteric liquid crystal induced by optical deformation of helix. *Phys. Rev. E* **69,** 061715 (2004).
41. Kogelnik, H. & Shank, C. V. Coupled-wave theory of distributed feedback lasers. *J. Appl. Phys.* **43,** 2327–2336 (1972).
42. Pershan, P. S. *Structure of Liquid Crystal Phases* (World Scientific, 1998).
43. Jen, S., Clark, N. A., Pershan, P. S. & Priestly, E. B. Polarized Raman scattering studies of orientational order in uniaxial liquid crystalline phases. *J. Chem. Phys.* **66,** 4635–4661 (1977).
44. Dunmur, D. *The Optics of Thermotropic Liquid Crystals* (ed. Elston, S. & Sambles, J. R.) Ch. 2 (Taylor and Francis, 1998).
45. Collings, P. J. & Hird, M. *Introduction to Liquid Crystals* (Taylor and Francis, 1997).
46. Oswald, P. & Pieranski, P. *Nematic and Cholesteric Liquid Crystals* (Taylor and Francis, 2005).
47. Oswald, P. & Pieranski, P. *Smectic and Columnar Liquid Crystals* (Taylor and Francis, 2006).
48. Stegemeyer, H., Blumel, T. H., Hiltrop, K., Onusseit, H. & Porsch. F. Thermodynamic, structural and morphological studies on liquid-crystalline blue phases. *Liq. Cryst.* **1,** 3–28 (1986).
49. Kikuchi, H., Yokota, M., Hisakado, Y., Yang, H. & Kajiyama, T. Polymer-stabilized liquid crystal blue phases. *Nature Mater.* **1,** 64–68 (2002).
50. Coles, H. J. & Pivnenko, M. N. Liquid crystal 'blue phases' with a wide temperature range. *Nature* **436,** 997–100 (2005).
51. de Vries, H. Rotatory power and other optical properties of certain liquid crystals. *Acta. Cryst.* **4,** 219–226 (1951).
52. Belyakov, V. A., Dmitrienko, V. E. & Orlov, V. P. Optics of cholesteric liquid crystals. *Sov. Phys. Uspekhi* **22,** 64–88 (1979).
53. Belyakov, V. A. & Dmitrienko, V. D. Theory of the optical properties of cholesteric liquid crystals. *Sov. Phys. Sol. State* **15,** 1811–1815 (1974).
54. Muñoz, A., Palffy-Muhoray, P. & Taheri, B. Ultraviolet lasing in cholesteric liquid crystals. *Opt. Lett.* **26,** 804–806 (2001).
55. Schmidtke, J. & Stille, W. Fluorescence of a dye-doped cholesteric liquid crystal film in the region of the stop band: theory and experiment. *Eur. Phys. J.* **31,** 179–194 (2003).
56. Cao, W., Palffy-Muhoray, P., Taheri, B., Marino, A. & Ab, G. Lasing thresholds of cholesteric liquid crystals lasers. *Mol. Cryst. Liq. Cryst.* **429,** 101–110 (2005).
57. Morris, S. M., Ford, A. D., Pivnenko, M. N. & Coles H. J. The effects of reorientation on the emission properties of a photonic band edge liquid crystal laser. *J. Opt. A* **7,** 215–223 (2005).
58. Wang, Y. *et al.* Dependence of lasing threshold power on excitation wavelength in dye-doped cholesteric liquid crystals. *Opt. Comm.* **280,** 408–411 (2007).
59. Woon, K. L., O'Neill, M., Richards, G. J., Aldred, M. P. & Kelly, S. M. Stokes parameter studies of spontaneous emission from chiral nematic liquid crystals as a one-dimensional photonic stopband crystal: Experiment and theory. *Phys. Rev. E* **71,** 041706 (2005).
60. Huang, Y. *et al.* Incident angle and polarization effects on the dye-doped cholesteric liquid crystal laser. *Opt. Comm.* **261,** 91–96 (2006).
61. Belyakov, V. A. Low threshold DFB lasing in chiral LC at diffraction of pumping wave. *Mol. Cryst. Liq. Cryst.* **453,** 43–69 (2006).
62. Matsuhisa, Y. *et al.* Low-threshold and high efficiency lasing upon band-edge excitation in a cholesteric liquid crystal. *Appl. Phys. Lett.* **90,** 091114 (2007).
63. Milner, V. & Genack, A. Z. Photon localization laser: Low-threshold lasing in a random amplifying layered medium via wave localization. *Phys. Rev. Lett.* **94,** 073901 (2005).
64. Shirota, K., Sun, H.-B. & Kawata. S. Two-photon lasing of dye-doped photonic crystal lasers. *Appl. Phys. Lett.* **84**, 1632–1634 (2004).
65. Chanishvili, A. *et al.* Laser emission from a dye-doped cholesteric liquid crystal pumped by another cholesteric liquid crystal laser. *Appl. Phys. Lett.* **85,** 3378–3880 (2004).
66. J, R. *et al.* Electrically switchable lasing from pyrromethene 597 embedded holographic-polymer dispersed liquid crystal. *Appl. Phys. Lett.* **85,** 6095–6097 (2004).
67. Wu, S.-T. & Fuh, A. Y.-G. Lasing in photonic crystals based on dye-doped holographic polymer-dispersed liquid crystal reflection gratings. *Jpn. J. Appl. Phys.* **44,** 977–980 (2005).
68. Liu, Y. J. *et al.* Low-threshold and narrow-linewidth lasing from dye-doped holographic polymer-dispersed liquid crystal transmission gratings. *Appl. Phys. Lett.* **88,** 061107 (2006).
69. Woltman, S. J. & Crawford G. P. Patterned liquid-crystal laser film for multi-dimensional multi-color emissive film technology. *J. Soc. Inf. Disp.* **15,** 559–564 (2007).
70. Jakubiak, R., Tondiglia, V. P., Natarajan, L. V., Lloyd, P. F. & Sutherland, R. Lasing of pyrromethene 597 in 2D holographic polymer dispersed liquid crystals: influence of columnar conformation. *Proc. SPIE* **7232,** 72320K (2009).
71. Blinov, L. M. *et al.* Electric field tuning a spectrum of nematic liquid crystal lasing with the use of a periodic shadow mask. *J. Nonlinear Opt. Phys.* **1,** 75–90 (2007).
72. Blinov, L. M., Cipparrone, G., Pagliusi, P., Lazarev, V. V. & Palto, S. P. Simple voltage tunable liquid crystal laser. *Appl. Phys. Lett.* **90,** 131103 (2007).
73. Blinov, L. M., Cipparrone, G., Pagliusi, P., Lazarev, V. V. & Palto, S. P. Mirrorless lasing from nematic liquid crystals in the plane waveguide geometry without refractive index or gain modulation. *Appl. Phys. Lett.* **89,** 031114 (2006).
74. Kopp, V. I. & Genack A. Z. Large coherence area thin-film stop-band lasers. *Phys. Rev. Lett.* **86**, 1753–1756 (2001).
75. Lee, C.-R. *et al.* Color cone lasing emission in a dye-doped cholesteric liquid crystal with a single pitch. *Opt. Express* **17,** 12910–12921 (2009).
76. Matsuhisa, Y., Ozaki, R., Takao, Y. & Ozaki, M. Linearly polarized lasing in one-dimensional hybrid photonic crystal containing cholesteric liquid crystal. *J. Appl. Phys.* **101,** 033120 (2007).
77. Morris, S. M., Ford, A. D., Pivnenko, M. N., Hadeler, O. & Coles, H. J. Correlations between the performance characteristics of a liquid crystal laser and the macroscopic material properties. *Phys. Rev. E* **74,** 061709 (2006).
78. Ford, A. D., Morris, S. M., Pivnenko, M. N., Gillespie, C. & Coles, H. J. Emission characteristics of a homologous series of bimesogenic liquid crystal lasers. *Phys. Rev. E* **76,** 051703 (2007).
79. Chee, M. G., Song, M. H., Kim, D., Takezoe, H. & Chung, I. J. Lowering lasing threshold in chiral nematic liquid crystal structure with different anisotropies. *Jpn. J. Appl. Phys.* **46,** L437–L439 (2007).
80. Araoka, F. *et al.* How doping a cholesteric liquid crystal with polymeric dye improves an order parameter and makes possible low threshold lasing. *J. Appl. Phys.* **94,** 279–283 (2003).
81. Shin, K.-C. *et al.* Advantages of highly ordered polymer-dyes for lasing in chiral nematic liquid crystals. *Jpn. J. Appl. Phys.* **43,** 631–636 (2004).
82. Dolgaleva, K. *et al.* Enhanced laser performance of cholesteric liquid crystals doped with oligofluorene dye. *J. Opt. Soc. Am. B* **25,** 1496–1504 (2008).
83. Chinelatto, L. S. *et al.* Oligofluorene blue emitters for cholesteric liquid crystal lasers. *J. Photochem. Photobio. A* **210,** 130–139 (2010).
84. Watanabe, Y. *et al.* Extremely low threshold in a pyrene-doped distributed feedback cholesteric liquid crystal laser. *Appl. Phys. Express* **2,** 102501 (2009).
85. Mowatt, C. *et al.* Comparison of the performance of photonic band-edge liquid crystal lasers using different dyes as the gain medium. *J. Appl. Phys.* **107,** 043101 (2010).
86. Coles, H. J., Morris, S. M., Hands, P. J. W., Choi, S. S. & Wilkinson, T. D. Red-green-blue tuneable liquid crystal laser devices. *Proc. SPIE* **7414,** 741402 (2009).
87. Huang, Y., Lin, T.-H., Zhou, Y. & Wu, S.-T. Enhancing the laser power by stacking multiple dye-doped chiral polymer films. *Opt. Express* **14,** 11299–11303 (2006).
88. Amemiya, K. *et al.* Lowering the lasing threshold by introducing cholesteric liquid crystal films to dye-doped cholesteric liquid crystal cell surfaces. *Jpn. J. Appl. Phys.* **44,** 7966–7971 (2005).
89. Zhou, Y., Huang, Y., Rapaport, A., Bass, M. & Wu, S.-T. Doubling the optical efficiency of a chiral liquid crystal laser using a reflector. *Appl. Phys. Lett.* **87,** 231107 (2005).
90. Blinov, L. M., Cipparrone, G., Lazarev, V. V. & Umanskii, B. A. Planar amplifier for a microlaser on a cholesteric liquid crystal. *Appl. Phys. Lett.* **91,** 061102 (2007).
91. Shtykov, N. M., Barnik, M. I., Blinov, L. M., Umanski, B. A. & Palto, S. P. Amplification of the lasing of a liquid-crystal microlaser by means of a uniform liquid-crystal layer. *JETP Lett.* **85,** 602–604 (2007).




© 2010 Macmillan Publishers Limited. All rights reserved

92. Blinov, L. M., Cipparrone, G., Mazzulla, A., Pagliusi, P. & Lazarev, V. V. Lasing in cholesteric liquid crystal cells: Competition of Bragg and leaky modes. *J. Appl. Phys*. **101,** 053104 (2007).
93. Blinov, L. M. *et al.* Quasi-in-plane leaky modes in lasing cholesteric liquid crystal cells. *J. Appl Phys.* **104,** 103115 (2008).
94. Strangi, G. *et al.* Color-tunable organic microcavity laser array using distributed feedback. *Phys. Rev. Lett.* **94,** 063903 (2005).
95. Hands, P. J. W., Morris, S. M., Wilkinson, T. D. & Coles, H. J. Two-dimensional liquid crystal laser array. *Opt. Lett.* **33,** 515–517 (2008).
96. Morris, S. M. *et al.* Polychromatic liquid crystal laser arrays towards display applications. *Opt. Express* **16,** 18827–18837 (2008).
97. Becchi, M., Ponti, S., Reyes, J. A. & Oldano, C. Defect modes in helical photonic crystals: An analytical approach. *Phys. Rev. B* **70,** 033103 (2004).
98. Jeong, S. M. *et al.* Defect mode lasing from a double-layered dye-doped polymeric cholesteric liquid crystal films with a thin rubbed defect layer. *Appl. Phys. Lett*. **90,** 261108 (2007).
99. Song, M. H. *et al.* Lasing from thick anisotropic layer sandwiched between polymeric cholesteric liquid crystal films. *Jpn. J. Appl. Phys*. **44,** 8165–8167 (2005).
100. Song, M. H. *et al.* Defect-mode lasing with lowered threshold in a three-layered hetero-cholesteric liquid-crystal structure. *Adv. Mater.* **18,** 193–197 (2006).
101. Song, M.-H. *et al.* Electrotunable non reciprocal laser emission from a liquid-crystal photonic device. *Adv. Funct. Mater*. **16,** 1793–1798 (2006).
102. Takanishi, Y. *et al.* Defect-mode lasing from a three-layered helical cholesteric liquid crystal structure. *Jpn. J. Appl. Phys*. **46,** 3510–3513 (2007).
103. Belyakov, V. A. Low threshold DFB lasing at the edge and defect modes in chiral liquid crystals. *Mol. Cryst. Liq. Cryst.* **488,** 279–308 (2008).
104. Ha, N. Y., Takanishi, Y., Ishikawa, K. & Takezoe, H. Simultaneous RGB reflections from single-pitched cholesteric liquid crystal films with Fibonaccian defects. *Opt. Express* **15,** 1024–1029 (2007).
105. Ha, N. Y. *et al.* Fabrication of a simultaneous red-green-blue reflector using single-pitched cholesteric liquid crystals. *Nature Mater*. **7,** 43–47 (2008).
106. Morris, S. M., Ford, A. D. & Coles, H. J. Removing the discontinuous shift in emission wavelength of a chiral nematic liquid crystal laser. *J. Appl. Phys.* **106,** 023112 (2009).
107. Chanishvili, A. *et al.* Widely tunable ultraviolet-visible liquid crystal laser. *Appl. Phys. Lett*. **86,** 051107 (2005).
108. Lin, T.-H. *et al.* Cholesteric liquid crystal laser with wide tuning capability. *Appl. Phys. Lett*. **86,** 161120 (2005).
109. Huang, Y., Zhou, Y. & Wu, S.-T. Spatially tunable laser emission in dye-doped photonic liquid crystals. *Appl. Phys. Lett.* **88,** 011107 (2006).
110. Huang, Y., Chen, L.-P., Doyle, C., Zhou, Y. & Wu, S.-T. Spatially tunable laser emission in dye-doped cholesteric polymer films. *Appl. Phys. Lett*. **89,** 111106 (2006).
111. Sonoyama, K., Takanishi, Y., Ishikawa, K. & Takezoe, H. Position-sensitive cholesteric liquid crystal dye laser covering a full visible range. *Jpn. J. Appl. Phys*. **46,** L874–L876 (2007).
112. Jeong, M.-Y., Choi, H. & Wu, J. W. Spatial tuning of laser emission in a dye-doped cholesteric liquid crystal wedge cell. *Appl. Phys. Lett*. **92,** 051108 (2008).
113. Wang, C.-T. & Lin, T.-H. Multi-wavelength laser emission in dye-doped photonic liquid crystals. *Opt. Express* **16,** 18334–18339 (2008).
114. Yoshida, H. *et al.* Position sensitive, continuous wavelength tunable laser based on photopolymerizable cholesteric liquid crystals with an in-plane helix alignment. *Appl. Phys. Lett.* **94,** 093306 (2009).
115. Chambers, M., Fox, M., Grell, M. & Hill, J. Lasing from a Förster transfer fluorescent dye couple dissolved in a chiral nematic liquid crystal. *Adv. Funct. Mater.* **12,** 808–810 (2002).
116. Sonoyama, K., Takanishi, Y., Ishikawa, K. & Takezoe, H. Lowering threshold by energy transfer between two dyes in cholesteric liquid crystal distributed feedback lasers. *Appl. Phys. Express* **1,** 032002 (2008).
117. Fuh, A. Y.-G. & Lin, T.-H. Lasing in chiral photonic liquid crystals and associated frequency tuning. *Opt. Express* **12,** 1857–1863 (2004).
118. Chanishvili, A. *et al.* Lasing in dye-doped cholesteric liquid crystals: Two new tuning strategies. *Adv. Mater.* **16,** 791–795 (2004).
119. Barnik, M. I. *et al.* Lasing from photonic structure: Cholesteric-voltage controlled nematic cholesteric liquid crystal. *J. Appl. Phys.* **103,** 123113 (2008).
120. Blinov, L. M. & Bartelino, R. (eds) *Liquid Crystal Microlaser* (Transworld Research Network, 2010).
121. Ford, A. D., Morris, S. M. & Coles, H. J. Photonics and lasing in liquid crystals. *Mater. Today* **9,** 36–42 (July–August, 2006).


## Additional information

The authors declare no competing financial interests.



© 2010 Macmillan Publishers Limited. All rights reserved